

# Valproic Acid Protects Motor Neuron Death by Inhibiting Oxidative Stress and Endoplasmic Reticulum Stress-Mediated Cytochrome C Release after Spinal Cord Injury

Jee Y. Lee,<sup>1,2</sup> Sejung Maeng,<sup>1</sup> So R. Kang,<sup>1,3</sup> Hye Y. Choi,<sup>1</sup> Tae H. Oh,<sup>1</sup> Bong G. Ju,<sup>4</sup> and Tae Y. Yune<sup>1–3,5</sup>

## Abstract

Both oxidative stress and endoplasmic reticulum (ER) stress are known to contribute to secondary injury, ultimately leading to cell death after spinal cord injury (SCI). Here, we showed that valproic acid (VPA) reduced cell death of motor neurons by inhibiting cytochrome c release mediated by oxidative stress and ER stress after SCI. After SCI, rats were immediately injected with VPA (300 mg/kg) subcutaneously and further injected every 12 h for an indicated time period. Motor neuron cell death at an early time after SCI was significantly attenuated by VPA treatment. Superoxide anion ( $O_2^-$ ) production and inducible NO synthase (iNOS) expression linked to oxidative stress was increased after injury, which was inhibited by VPA. In addition, VPA inhibited c-Jun N-terminal kinase (JNK) activation, which was activated and peaked at an early time after SCI. Furthermore, JNK activation and c-Jun phosphorylation were inhibited by a broad-spectrum reactive oxygen species (ROS) scavenger, Mn (III) tetrakis (4-benzoic acid) porphyrin (MnTBAP), indicating that ROS including  $O_2^-$  increased after SCI probably contribute to JNK activation. VPA also inhibited cytochrome c release and caspase-9 activation, which was significantly inhibited by SP600125, a JNK inhibitor. The levels of phosphorylated Bim and Mcl-1, which are known as downstream targets of JNK, were significantly reduced by SP600125. On the other hand, VPA treatment inhibited ER stress-induced caspase-12 activation, which is activated in motor neurons after SCI. In addition, VPA increased the Bcl-2/Bax ratio and inhibited CHOP expression. Taken together, our results suggest that cell death of motor neurons after SCI is mediated through oxidative stress and ER stress-mediated cytochrome c release and VPA-inhibited cytochrome c release by attenuating ROS-induced JNK activation followed by Mcl-1 and Bim phosphorylation and ER stress-coupled CHOP expression.

**Key words:** Bcl-2; cytochrome c; JNK; oxidative stress; SCI

## Introduction

**T**RAUMATIC SPINAL CORD INJURY (SCI) induces massive cell death through immediate cell death by necrosis and prolonged apoptotic cell death resulting from secondary injury, leading to permanent neurological deficits.<sup>1–3</sup> Secondary injury includes disturbances in ionic homeostasis, local edema, focal hemorrhage, excitotoxicity, oxidative stress, inflammation, and endoplasmic reticulum (ER) stress. Ventral horn motor neurons (VMN) are more vulnerable than other spinal neurons to acute SCI<sup>4</sup> and to neurodegenerative diseases such as amyotrophic lateral sclerosis (ALS).<sup>5,6</sup>

After SCI, reactive oxygen species (ROS), including superoxide anion ( $O_2^-$ ) and nitric oxide (NO) produced by NO synthases, especially by inducible NO synthase (iNOS), are increased and also mediate secondary injury, resulting in oxidative stress.<sup>7–10</sup> Oxida-

tive stress has been implicated in the pathogenesis of motor neuron death in animal models of SCI, familial ALS, traumatic brain injury, and cerebral ischemia.<sup>11–14</sup> Mitochondrial damage under oxidative stress leads to cytochrome c release, which activates the caspase cascades, leading to apoptotic cell death.<sup>7,15,16</sup> The ER is a subcellular organelle maintaining intracellular calcium homeostasis and proper folding of newly synthesized secretory and membranous proteins. Under the various cellular stresses, unfolded proteins are accumulated in ER and unfolded protein response (UPR) is initiated to restore normal ER function.<sup>7,17</sup> One pathway of UPR is the suppression of protein translation by inactivation of eukaryotic initiation factor (eIF), such as eIF-2 $\alpha$ , to prevent further accumulation of unfolded proteins. Another pathway is the upregulation of ER-localized chaperones, such as GRP78 and GRP94, to repair unfolded proteins. If the stress is prolonged, or the adaptive response fails, apoptotic cell death through the activation of

<sup>1</sup>Age-Related and Brain Diseases Research Center, <sup>2</sup>Neurodegeneration Control Research Center, <sup>3</sup>Graduate Program for Neuroscience, and <sup>5</sup>Department of Biochemistry and Molecular Biology, School of Medicine, Kyung Hee University, Korea.

<sup>4</sup>Department of Life Science, Sogang University, Seoul, Korea.

ER-associated caspase-12 occurs.<sup>18</sup> Several reports show that ER stress-mediated apoptotic cell death proceeds in the spinal cord after transient ischemia and traumatic injury.<sup>19–21</sup> Especially, several lines of evidences show that mitochondrial damage is coupled with ER stress-mediated apoptotic cell death.<sup>22,23</sup>

Valproic acid (VPA), a short-chain fatty acid, is widely used for the treatment of seizures and bipolar mood disorder.<sup>24,25</sup> A growing body of reports shows that VPA exerts neuroprotective effects against a variety of insults *in vitro* and *in vivo*. For example, VPA prevents cortical neuronal cell death from ischemia<sup>26,27</sup> and protects spinal motor neurons in animal models of spinal muscular atrophy or ALS.<sup>28,29</sup> In addition, VPA inhibits apoptotic cell death after SCI by attenuating blood–spinal cord barrier (BSCB) disruption,<sup>30</sup> and by inhibiting ER stress.<sup>31,32</sup> However, the mechanisms underlying the protective effect of VPA on ER stress- and oxidative stress-induced cell death after SCI have not been elucidated yet. Here, we show that VPA inhibits cytochrome c release by inhibiting ROS-dependent c-Jun N-terminal kinase (JNK) activation under oxidative stress, and reducing caspase-12 activation and CHOP expression under ER stress after SCI.

## Methods

### SCI

Adult rats (Sprague–Dawley; male; 250–300 g; Sam: TacN [SD] BR, Samtako, Osan, Korea) were anesthetized with chloral hydrate (500 mg/kg, i.p.), and a laminectomy was performed at the T9–T10 level exposing the cord beneath without disrupting the dura. The spinous processes of T8 and T11 were then clamped to stabilize the spine, and the exposed dorsal surface of the cord was subjected to moderate contusion injury (10 g x 25 mm) using an NYU impactor as previously described.<sup>33</sup> Sham-operated controls animals underwent a T10 laminectomy without weight-drop injury. All surgical interventions and postoperative animal care were performed in accordance with the Guidelines and Policies for Rodent Survival Surgery provided by the Animal Care Committee of the Kyung Hee University.

### Drug administration

VPA sodium salt (Sigma, St. Louis, MO) was dissolved in sterile phosphate-buffered saline (PBS) and injected subcutaneously into the animals.<sup>27,30</sup> Rats were given VPA (300 mg/kg) immediately after SCI, and then were injected with a same dose every 12 h for indicated time period. Both a JNK inhibitor, SP600125 (Merk Calbiochem, Darmstadt, Germany), and a broad-spectrum ROS scavenger, Mn (III) tetrakis (4-benzoic acid) porphyrin (MnTBAP, Merk Calbiochem) were dissolved in 2% dimethyl sulfoxide (DMSO) and normal saline, respectively. SP600125 (10 µg/250 g) and MnTBAP (2.5 mg/kg) were administered through intraspinal injection with 5 or 10 µL at 5 min after SCI. The dose of drugs used in the experiment was chosen based on previous research.<sup>34,35</sup> Intraspinal injection was performed as previously described.<sup>36</sup> In brief, SP600125 (5 µL) or MnTBAP (10 µL) was injected into the lesion epicenter (1.5 mm depth) using a pulled glass capillary pipette micropipette attached to a Hamilton syringe connected to a micromanipulator. The injection rate was 0.5 µL/min. Control groups received an equivolumetric injection of 2% DMSO or saline at the corresponding time points. No significant side effects resulting from VPA treatment, such as changes in body weight or an increase in mortality, were observed throughout our experiments.

### Tissue preparation

At indicated time points after SCI, animals were anesthetized with chloral hydrate (500 mg/kg) and perfused via cardiac puncture

initially with 0.1 M PBS, pH 7.4, and, subsequently, with 4% paraformaldehyde in 0.1 M PBS, pH 7.4. A 20 mm section of the spinal cord, centered at the lesion site, was dissected out, post-fixed by immersion in the same fixative for 5 h, and placed in 30% sucrose in 0.1 M PBS, pH 7.4. The segment was embedded in OCT for frozen sections, and longitudinal or transverse sections were then cut at 10 or 20 µm on a cryostat (CM1850; Leica, Germany).

### Cell counting of VMN

Three days after injury, we assessed the number of VMN as in our previous report.<sup>16</sup> Serial transverse sections (20 µm thickness) were collected every millimeter rostral and caudal 4 mm to the lesion site, and stained with cresyl violet acetate ( $n=5$ ). After determination of the cells located in the lower ventral horn, cells larger than half of the sampling square (20 × 20 µm) were counted as a VMN. The cells above the line at 150 µm ventral from the central canal were excluded. The cells were manually counted from each field using Metamorph software (molecular devices).

### Terminal deoxynucleotidyl transferase-mediated deoxyuridine triphosphate-biotin nick end labeling (TUNEL)

One day after injury, serial spinal cord sections (20 µm thickness) were collected and processed for TUNEL according to the manufacturer's instruction (Millipore, Billerica, MA). The negative control sections were treated similarly, but incubated in the absence of terminal deoxynucleotidyl transferase (TdT) enzyme, dUTP-digoxigenin, or anti-digoxigenin antibody, and the positive control sections were incubated in DNaseI. Only those cells showing morphological features of nuclear condensation and/or compartmentalization only in the gray matter (GM) were counted as TUNEL positive. For quantification, serial transverse sections (20 µm thickness) were collected every 100 µm from 2 mm rostral to 2 mm caudal to the lesion epicenter for neurons (total 40 sections,  $n=5$ ). As described in a previous report,<sup>37</sup> the region of maximal spinal cord damage was determined by examination of tissue loss with serial sections at the so-called "lesion epicenter." To avoid any bias in the results, cell counts were performed blind by persons who did not know the treatment history of the animals; no results were revealed to the counters until the completion of data collection for the entire study.

### In situ detection of superoxide anion

The production of superoxide anion  $O_2^-$  after SCI was examined by the *in situ* detection of oxidized hydroethidine (HEt) as described.<sup>15</sup> HEt is oxidized to the fluorescent ethidium (Etd) by  $O_2^-$ <sup>38</sup> and is considered as an indicator of intracellular  $O_2^-$ . After SCI, HEt (Invitrogen, Carlsbad, CA; stock solution 100 mg/mL) in DMSO was diluted to 1 mg/mL in PBS just before use, and 200 µL of HEt was injected intravenously 1 h before the animals were killed ( $n=4$ ). At 4 h after injury, spinal cord sections were prepared. The fluorescence was assessed microscopically at Ex = 510–550 nm and Em > 580 nm for Etd detection, and photographed with an Olympus microscope (BX51, Olympus, Japan) with software accompanying the Cool SNAP camera (Roper Scientific, Sarasota, FL). For quantitative analysis of Etd fluorescence, the area of tissue fluorescence in three coronal sections at an interval of 30 µm at a distance of 2 mm from the lesion epicenter was analyzed using Image MetaMorph software (Molecular devices, Sunnyvale, CA) as described.<sup>15</sup>

### Immunohistochemistry

Frozen sections were processed for double immunofluorescence staining with antibodies against nitrotyrosin (1:1000, Millipore), phosphorylated-Jun N-terminal kinase (p-JNK; 1:500, Cell

Signaling Technology, Danvers, MA), caspase-12 (1:100, Santa Cruz Biotechnology, Santa Cruz, CA), and antibody specific for neurons (NeuN; 1:100, Millipore) as described.<sup>39</sup> After three washes with PBS for 15 min, sections were blocked with 5% normal serum in PBS with Tween (PBS-T) (0.1% Triton X-100) for 1 h at room temperature and then incubated with primary antibodies overnight at 4°. After washing with PBS-T three times, FITC or cy3-conjugated secondary antibodies (Jackson ImmunoResearch, West Grove, PA) were incubated for 1 h at room temperature. Nuclei were labeled with 4',6-diamidino-2-phenylindole (DAPI) according to the protocol of the manufacturer (Molecular Probes, Eugene, OR). In all controls, primary antibody was omitted, or the primary antibody was replaced with a non-immune control antibody.

#### Western blot

To prepare total protein, segments of spinal cord (1 cm) including the lesion site, were homogenized in a lysis buffer containing 1% Nonidet P-40, 20 mM Tris, pH 8.0, 137 mM NaCl, 0.5 mM ethylenediaminetetraacetic acid (EDTA), 10% glycerol, 10 mM Na<sub>2</sub>P<sub>2</sub>O<sub>7</sub>, 10 mM NaF, 1 μg/mL aprotinin, 10 μg/mL leupeptin, 1 mM vanadate, and 1 mM phenylmethanesulfonyl fluoride (PMSF). Tissue homogenates were incubated for 20 min at 4°C and centrifuged at 25,000g for 30 min at 4°C. Protein extraction of cytosolic fractions (S-100) was performed as previously described.<sup>40</sup> In brief, the tissues resuspended in a homogenizing

buffer containing 10 mM PBS, pH 7.5, and 250 mM sucrose, and homogenized in a Dounce homogenizer. Tissue homogenate was centrifuged at 200g for 10 min at 4°C, and the supernatant was centrifuged at 8000g for 10 min at 4°C. The supernatant was centrifuged at 40,000g for 1 h at 4°C, and the supernatant was used as S-100. Protein concentration was determined using the bicinchoninic acid (BCA) protein assay reagent (Pierce, Rockford, IL). Total (50 μg) or S-100 (30 μg) protein was separated by sodium dodecyl sulfate (SDS)-polyacrylamide gel electrophoresis (PAGE) and transferred to nitrocellulose membranes (Millipore) by electrophoresis. The membranes were then incubated with antibodies against caspase-12 (1:500, Santa Cruz Biotechnology), caspase-9 (1:500, Cell Signaling Technology), Caspase-3 (1:200, Cell Signaling Technology), CHOP (1:1,000, Santa Cruz Biotechnology), cytochrome c (1:500, Santa Cruz Biotechnology), Bcl-2 (1:500, Santa Cruz Biotechnology), nitrotyrosine (1:500, Millipore), Bax (1:500, Santa Cruz Biotechnology), phosphorylated-Bim (p-Bim; 1:500, Bioss, Woburn, MA), Bim (1:500, Santa Cruz Biotechnology), myeloid cell leukemia 1 (Mcl-1, 1:500, Pharmingen, San Diego, CA), phosphorylated-Mcl-1 (p-Mcl-1; 1:500, Bioss), iNOS (1:1,000, Transduction Laboratory, Lexington, KY), JNK (1:500, Cell Signaling Technology), p-JNK (1:500, Cell Signaling Technology), p-c-Jun (1:1000, Cell signaling Technology), c-Jun (1:500, Santa Cruz Biotechnology), and hydroxynonenal (HNE) (1:1,000, Alpha diagnostic, San Antonio, TX). The primary antibodies were detected with horseradish peroxidase-conjugated secondary antibodies (Jackson ImmunoResearch). Immunoreactive

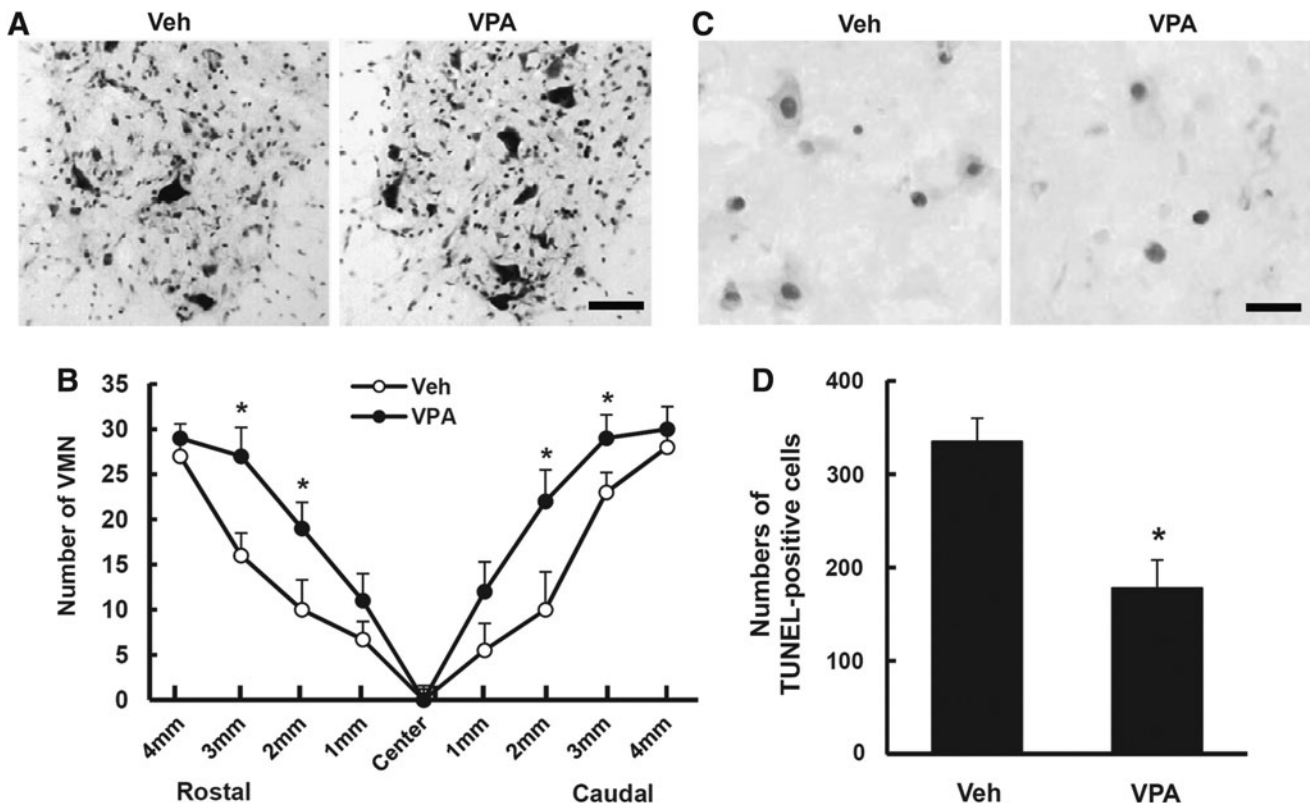


**FIG. 1.** Valproic acid (VPA) inhibits cell death of ventral motor neurons (VMN) after spinal cord injury (SCI). VPA (300 mg/kg) was injected subcutaneously into the rats after SCI and spinal tissues were isolated at 1 day for Terminal deoxynucleotidyl transferase-mediated deoxyuridine triphosphate-biotin nick end labeling (TUNEL) and 3 days for Nissl staining and counting ( $n = 5/\text{group}$ ). (A) Representative Nissl staining showing ventral horn of spinal cord 2 mm rostral from lesion site. Scale bar, 50 μm. (B) Counting analysis of VMN from 4 mm to 4 mm rostral and caudal from lesion site. (C) Representative TUNEL staining with injured spinal tissue 1 mm rostral from lesion site. Scale bar, 30 μm. (D) Quantification of TUNEL-positive cells in the ventral horn from 2 mm to 2 mm rostral and caudal from lesion site. Note that VPA significantly inhibited VMN cell loss and cell death after SCI. Data represent the mean  $\pm$  SD. \* $p < 0.05$ .

bands were visualized by chemiluminescence using Supersignal (Thermo scientific, Rockford, IL).  $\beta$ -Tubulin (1:10,000; Sigma) was used as an internal control. Experiments were repeated three times and the densitometric values of the bands on Western blots obtained by AlphaImager software (Alpha Innotech Corporation, San Leandro, CA) were subjected to statistical analysis. Background in films was subtracted from the optical density measurements.

#### RNA isolation and reverse transcription polymerase chain reaction (RT-PCR)

Total RNA was isolated using TRIZOL Reagent (Invitrogen), and 0.5  $\mu$ g of total RNA was reverse-transcribed into first strand cDNA using Moloney murine leukemia virus (MMLV) according to the manufacturer's instructions (Invitrogen). For PCR amplifications, the following reagents were added to 1  $\mu$ L of first strand cDNA: 0.5 U taq polymerase (Takara, Kyoto, Japan), 20 mM Tris-HCl, pH 7.9, 100 mM KCl, 1.5 mM MgCl<sub>2</sub>, 250  $\mu$ M dNTP, and 10 pmole of each specific primer. PCR conditions were as follows: denaturation at 94°C, 30 sec, primer annealing at indicated temperature, 30 sec, and amplification at 72°C, 30 sec. PCR was terminated by incubation at 72°C for 7 min. The primers used for CHOP, iNOS, and glyceraldehyde 3-phosphate dehydrogenase (GAPDH) were synthesized by the Genotech (Daejeon, Korea), and the sequences of the primers are as follows (5'-3'): CHOP forward,

5'-CCA GCA GAG GTC ACA AGC AC-3'; CHOP reverse, 5'-CGC ACT GAC CAC TCT GTT TC-3' (127 bp, 64°C for 30 cycles); iNOS forward, 5'- CTC CAT GAC TCT CAG CAC AGA G-3'; iNOS reverse, 5'- GCA CCG AAG ATA TCC TCA TGA T-3' (401 bp, 56°C for 25 cycles); GAPDH forward, 5'- TCC CTC AAG ATT GTC AGC AA-3'; GAPDH, reverse, 5'-AGA TCC ACA ACG GAT ACA TT-3' (308 bp, 50°C for 23 cycles). The plateau phase of the PCR reaction was not reached under these PCR conditions. After amplification, PCR products were subjected to a 1.5-2% agarose gel electrophoresis and visualized by ethidium bromide staining. The relative density of bands (relative to sham value) was analyzed by the AlphaImager software (Alpha Innotech Corporation, San Leandro, CA). Experiments were repeated three times and the values obtained for the relative intensity were subjected to statistical analysis. The gels shown in the figures are representative of results from three separate experiments.

#### Statistical analysis

Data are presented as the mean  $\pm$  SD values. Comparisons between vehicle- and VPA-treated groups were made by unpaired Student's *t* test. Multiple comparisons between groups were performed with one way ANOVA. Statistical significance was accepted with *p* < 0.05. Statistical analyses were performed using SPSS 15.0 (SPSS Science, Chicago, IL).

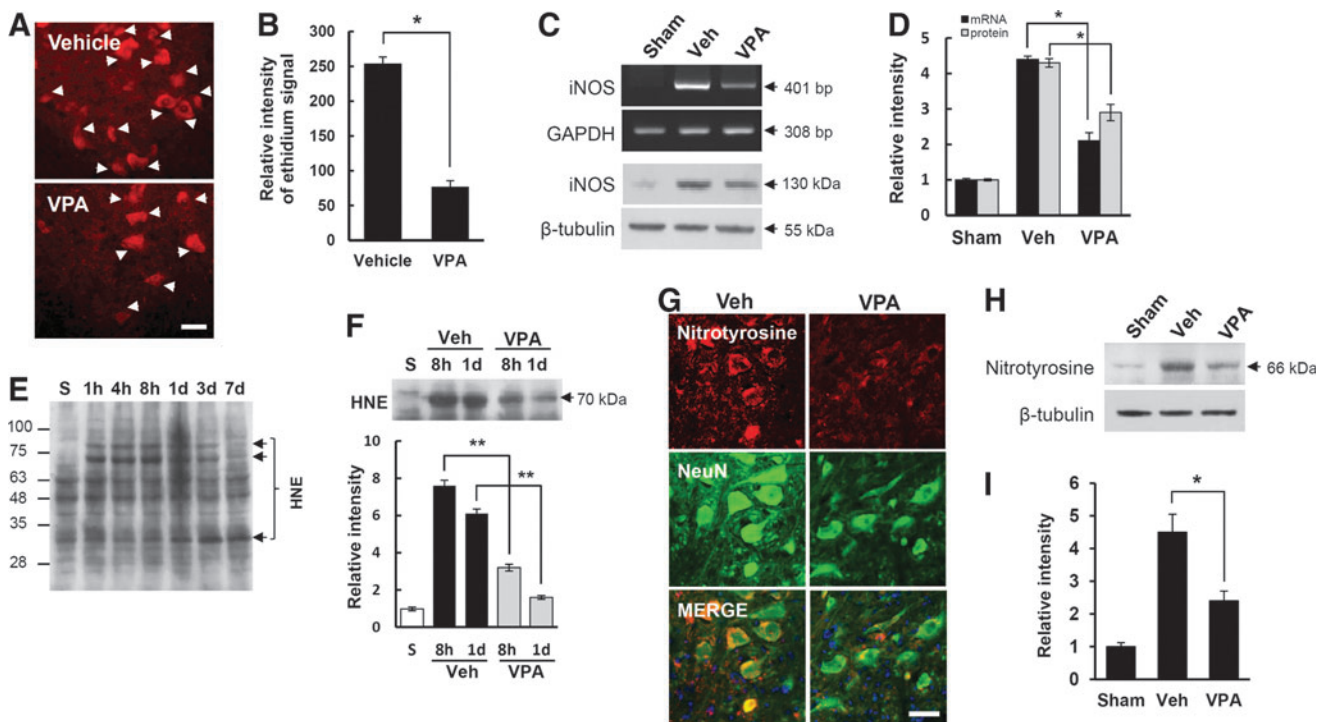


**FIG. 2.** Valproic acid (VPA) inhibits reactive oxygen species (ROS) production and inducible NO synthase (iNOS) expression after spinal cord injury (SCI). Injured rats treated with and without VPA were injected with 200  $\mu$ L of hydroethidine (HET) (1 mg/mL) and spinal cord tissues were harvested at 4 h after injury (*n* = 4/group). (A) Representative photomicrographs of HET fluorescence from the spinal sections taken 2 mm rostral to the lesion epicenter. Arrows indicate HET-positive neurons in the gray matter (GM). Scale bar, 25  $\mu$ m. (B) Quantitative analysis of relative ethidium fluorescence intensity. Spinal samples treated with and not treated with VPA were harvested at 4 h after injury (*n* = 3/group) and then iNOS expression was examined by reverse transcription polymerase chain reaction (RT-PCR) (C, upper), Western blot (C, lower), and quantitative analysis (D). Note that superoxide anion production and iNOS expression were significantly inhibited by VPA after SCI. Total proteins and tissues treated with and not treated with VPA after SCI were prepared at indicated time points. (E and F upper) Western blots and quantification analysis (F lower) of hydroxynonenal (HNE) (*n* = 3/group), (G) double staining with anti-nitrotyrosine and anti-NeuN antibodies, Western blots (H) and quantification analysis (I) of nitrotyrosine at 1 day after injury (*n* = 3/group). Note that VPA significantly decreased SCI-induced increase of HNE at 8 h and 1 day after injury. VPA also alleviated immunoreactivity of nitrotyrosine in the VMN at 1 day after injury. Scale bar, 30  $\mu$ m. Data represent the mean  $\pm$  SD. \**p* < 0.05, \*\**p* < 0.01. Color image is available online at [www.liebertpub.com/neu](http://www.liebertpub.com/neu)

## Results

### VPA inhibits motor neuron cell death after SCI

VPA is known to alleviate oxidative damage to lipids and protein in primary cultured rat cortical cells.<sup>41</sup> As motor neuron cell death occurs at an early stage after SCI, and ROS play important roles in the VMN cell death,<sup>16</sup> we first examined the effect of VPA on the loss of motor neurons in the ventral horn by Nissl staining and counting the neurons. Serial transverse sections of the spinal cord were stained with cresyl violet, and VMN were counted. As in our previous report,<sup>15</sup> a massive loss of VMN was observed in the lesion area at 3 days after injury ( $n=5$ , Fig. 1A). Furthermore, the loss of VMN rostrally and caudally from the lesion site was significantly alleviated in VPA-treated groups as compared with vehicle controls (Fig. 1B,  $p<0.05$ ). To examine whether the loss of VMN may be mediated through cell death, we performed TUNEL staining and counting analysis. As shown in Figure 1C, TUNEL-positive cells were observed in the ventral horn at 1 day after SCI. In addition, quantification analysis of TUNEL-positive cells (2 mm rostral to 2 mm caudal from lesion site, total 40 sections) shows that the cell death of VMN was significantly inhibited by VPA when compared with vehicle control ( $n=5$ , vehicle,  $335 \pm 25$  vs. VPA,  $178 \pm 30$ ,  $p<0.05$ ).

### VPA inhibits superoxide anion production and iNOS expression after SCI

ROS are produced excessively, and contribute to secondary injury, leading to apoptotic cell death after SCI.<sup>4,7,15,16</sup> As VPA is

known to alleviate oxidative damage to lipids and protein in primary cultured rat cortical cells,<sup>41</sup> we examined whether VPA would inhibit ROS production and thereby alleviate oxidative damage after SCI. To detect  $O_2^-$ , a specific indicator of  $O_2^-$ , HET fluorescent dye (200  $\mu\text{g}/250\text{ g}$ ), was injected in injured rats treated with and not treated with VPA. Strong HET fluorescence was observed in the cytoplasm of VMN and interneurons at 4 h after injury (Fig. 2A) as in our previous report,<sup>42</sup> whereas no fluorescence was observed in uninjured sham controls (data not shown). In addition, HET fluorescence in VMN appeared as punctated in the cytoplasm upon higher magnification, suggesting the presence of  $O_2^-$  in mitochondria (data not shown). In particular, quantitative analysis showed that the relative intensity of Etd fluorescence was significantly lower in the VPA-treated groups than that in the vehicle control groups ( $n=4$ , Fig. 2B; vehicle,  $254 \pm 9.5$  vs. VPA,  $77 \pm 8.8$  at 4 h,  $p<0.05$ ) (Fig. 2B). Our previous report also showed that the expression of iNOS following NO production is increased, and known to contribute to oxidative stress after SCI.<sup>8</sup> Therefore, we examined the effect of VPA on iNOS expression at 4 h after SCI by RT-PCR and Western blot. As shown in Fig. 2C, both iNOS mRNA (upper panel) and protein expression (bottom panel) were increased after SCI, which were inhibited by VPA treatment. Quantitative analysis showed that VPA significantly decreased the expression of iNOS mRNA and protein as compared with vehicle control ( $n=3$ , Fig. 2D; vehicle,  $4.4 \pm 0.09$  vs. VPA,  $2.1 \pm 0.23$  for mRNA; vehicle,  $4.3 \pm 0.12$  vs. VPA,  $2.9 \pm 0.23$  for protein,  $p<0.05$ ). These results indicate that VPA inhibits SCI-induced ROS production and iNOS expression.

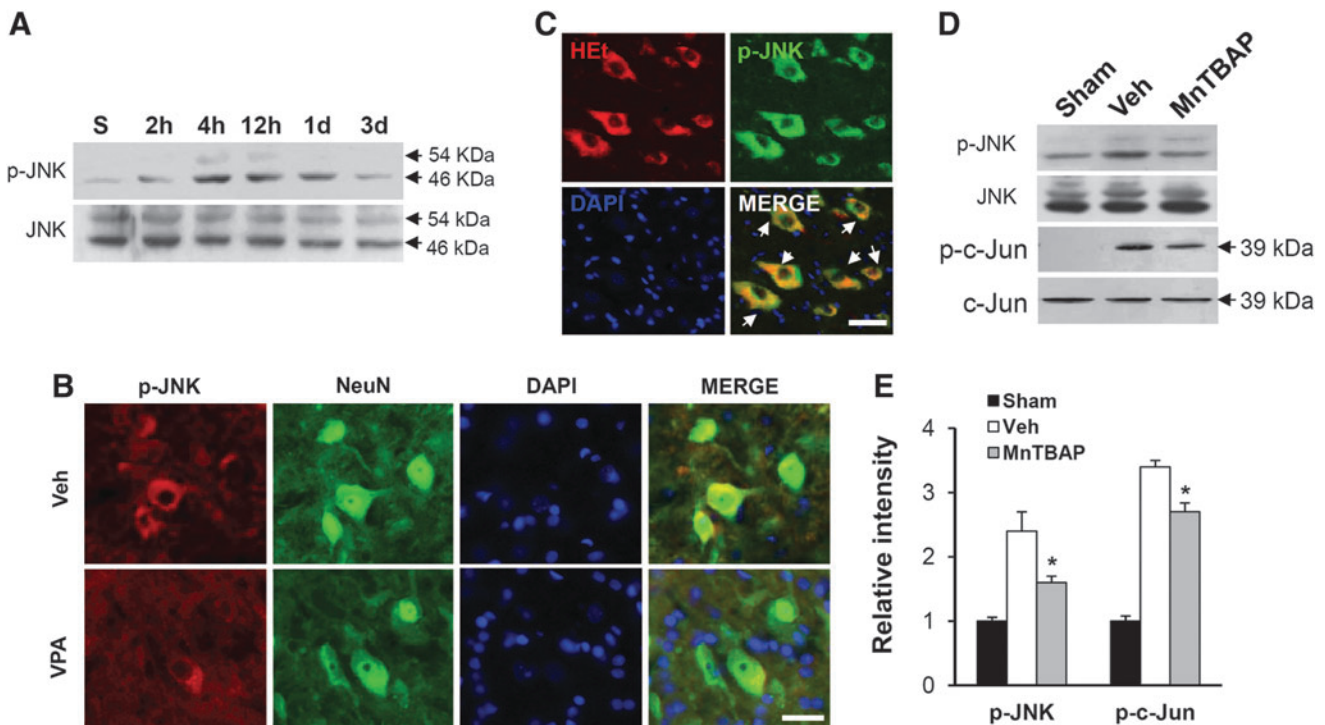


**FIG. 3.** Reactive oxygen species (ROS) induced c-Jun N-terminal kinase (JNK) activation in the ventral motor neurons (VMN) after spinal cord injury (SCI). Spinal total protein and tissue were prepared at indicated time points after SCI. Western blot of p-JNK (A) at 2 h, 4 h, 12 h, 1 day, and 3 days after injury, and double immunostaining (B) with anti-p-JNK and anti-NeuN antibodies using injured coronal tissue at 4 h after injury. Note that the level of p-JNK was increased and peaked at 4–12 h after injury, and that p-JNK was co-localized in neurons, especially in VMN. Valproic acid (VPA) also alleviated immunoreactivity of p-JNK in the VMN after injury. (C) Immunofluorescence staining of p-JNK with hydroethidine (HEt)-injected tissue. Western blots (D) and quantification analysis (E) of p-JNK and p-c-Jun with samples (at 4 h after injury) treated with Mn (III) tetrakis (4-benzoic acid) porphyrin (MnTBAP) (2.5 mg/kg,  $n=3/\text{group}$ ). Note that the level of p-JNK and p-c-Jun increased after SCI was significantly decreased by MnTBAP. Data represent the mean  $\pm$  SD. \* $p<0.05$ . Color image is available online at [www.liebertpub.com/neu](http://www.liebertpub.com/neu)

It is also well known that ROS induce damage to macromolecules such as proteins, lipids, and DNA, resulting in functional impairments of these molecules.<sup>43</sup> Therefore, we examined the effect of VPA on ROS-mediated damage of macromolecules. As shown in Figs. 2E–G, the level of HNE (at 8 h and 1 day after injury) and the intensity of nitrotyrosine immunoreactivity (at 1 day after injury) in the VMN were increased after SCI, suggesting that both lipid peroxidation and protein nitration by ROS were increased after SCI. Furthermore, VPA significantly decreased lipid peroxidation and protein nitration as compared with vehicle control ( $n=3$ , Figs. 2F and 2I; vehicle,  $7.6 \pm 0.3$  vs. VPA,  $3.2 \pm 0.18$  at 8 h; vehicle,  $6.1 \pm 0.25$  vs. VPA,  $1.6 \pm 0.1$  at 1 day for HNE,  $p < 0.01$ ; Fig. 2I; vehicle,  $4.5 \pm 0.55$  vs. VPA,  $2.4 \pm 0.3$ ,  $p < 0.05$ )

#### VPA inhibits ROS-dependent JNK activation after SCI

It is known that under the oxidative stress and ER stress, JNK is activated,<sup>44,45</sup> and contributes to apoptotic cell death after SCI.<sup>46,47</sup> Therefore, we examined the effect of ROS on JNK activation after SCI. Spinal samples were prepared from injured spinal cords immediately treated with and not treated with MnTBAP (2.5 mg/kg) after injury and isolated at indicated time points. As shown in Figure 3A, the level of p-JNK was increased at early times (4 and 12 h) after SCI. Double staining also showed that the immunoreactivity for p-JNK was observed in the VMN of spinal ventral horn (Fig. 3B). In addition, p-JNK was co-localized in HET positive VMN (Fig. 3C). Furthermore, JNK activation was significantly inhibited in the MnTBAP-treated group as compared with the vehicle-treated group ( $n=3$ , vehicle,  $2.4 \pm 0.3$  vs. VPA,  $1.6 \pm 0.1$ ,  $p < 0.05$ ). The level of p-c-Jun, a downstream molecule of JNK, was

also significantly decreased by MnTBAP treatment as compared with vehicle control (Figs. 3D and E) ( $n=3$ , vehicle,  $3.4 \pm 0.1$  vs. MnTBAP,  $2.7 \pm 0.2$ ,  $p < 0.05$ ). Next, to examine the effect of VPA on JNK activation after injury, spinal samples were prepared from injured spinal cords treated with and not treated with VPA, and Western blots of p-JNK and p-c-Jun were processed. As shown in Figure 4, VPA significantly inhibited JNK activation and c-Jun phosphorylation after SCI when compared with vehicle control ( $n=3$ , p-JNK, vehicle,  $2.7 \pm 0.23$  vs. VPA,  $1.4 \pm 0.2$ ,  $p < 0.05$ ; p-c-Jun, vehicle,  $3.8 \pm 0.23$  vs. VPA,  $1.36 \pm 0.14$  at 4 h,  $p < 0.01$ ). The levels of total JNK and c-Jun were not changed (data not shown). These results suggest that ROS are involved in JNK activation after SCI, and that VPA inhibits JNK activation at least in part by reducing ROS production.

#### VPA inhibits cytochrome c release and caspase-9 activation after SCI

After SCI, cytochrome c is released and mitochondria-dependent caspase-9 activation follows, resulting in apoptotic cell death of VMN.<sup>48,49</sup> Therefore, we examined whether VPA would inhibit cytochrome c release and caspase-9 activation after SCI. S-100 proteins were prepared from injured spinal cords treated with and not treated with VPA (300 mg/kg) isolated at 4 h after injury, and were subjected to Western blotting. As shown in Figure 5, cytochrome c release into cytoplasm from mitochondria was markedly increased after SCI as reported,<sup>33</sup> and its release was significantly attenuated by VPA treatment ( $n=3$ , vehicle,  $3.8 \pm 0.18$  vs. VPA,  $1.4 \pm 0.21$ ,  $p < 0.05$ ). VPA treatment also significantly reduced the level of caspase-9 after injury when compared with the

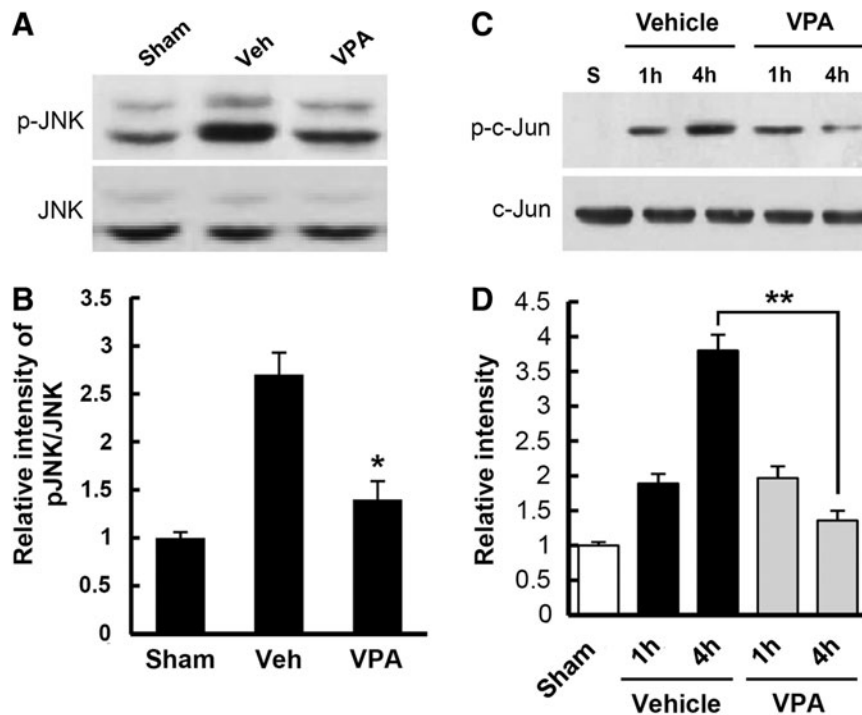


**FIG. 4.** Valproic acid (VPA) inhibits c-Jun N-terminal kinase (JNK) activation after spinal cord injury (SCI). Total protein was prepared from spinal tissues treated with and not treated with VPA at 1 and/or 4 h after SCI, and Western blots of p-JNK, JNK, p-c-Jun, and c-Jun were performed ( $n=3$ /group). Western blots (A) and quantification analysis (B) of p-JNK and JNK at 4 h after injury. Note that SCI-induced JNK activation was significantly inhibited by VPA. Western blots (C) and quantification analysis (D) of p-c-Jun and c-Jun at 1 and 4 h after injury. Note that the level of p-c-Jun was increased after injury and significantly decreased by VPA at 4 h as compared with vehicle control. Data represent the mean  $\pm$  SD. \* $p < 0.05$ , \*\* $p < 0.01$ .

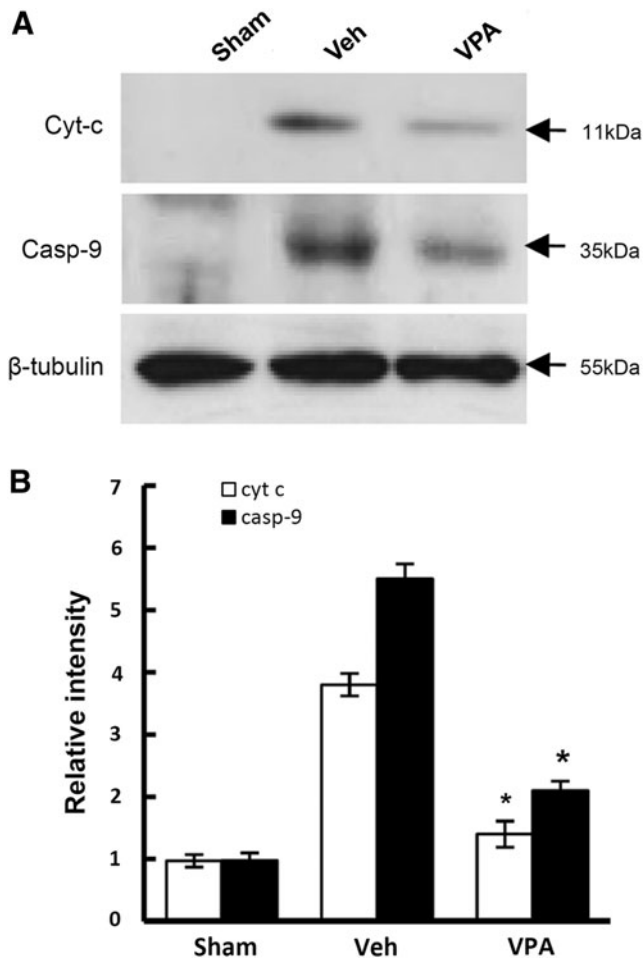


**FIG. 5.** Valproic acid (VPA) inhibits cytochrome c release and caspase-9 activation after spinal cord injury (SCI). After SCI, rats was immediately given with VPA (300 mg/kg) and fractioned cytoplasmic protein (S-100) were prepared at 4h after injury as described in Methods section ( $n=3$ /group). S-100 (30  $\mu$ g) were processed for Western blots of cytochrome c and caspase-9 (**A**) and quantification (**B**) Note that VPA significantly decreased the level of cytochrome c released into the cytoplasm, and activated caspase-9 at 4h after injury as compared with vehicle. Values are mean  $\pm$  SD. \* $p < 0.05$ .

vehicle-treated control ( $n=3$ , vehicle,  $5.5 \pm 0.24$  vs. VPA,  $2.1 \pm 0.15$ ,  $p < 0.05$ ).

#### JNK activation mediates Mcl-1 and Bim phosphorylation after SCI

JNK is activated under oxidative stress, and is known to mediate cytochrome c release leading to apoptotic cell death.<sup>50,51</sup> In addition, our data showed that VPA inhibited cytochrome c release (see Fig. 5) and ROS-induced JNK activation (see Fig. 4). Therefore, to examine whether the inhibition of JNK activation by VPA would influence cytochrome c release from mitochondria, SP600125 (10  $\mu$ g/250 g), a specific JNK inhibitor, was injected into injured spinal cord after injury. SP600125 is a reversible adenosine triphosphate (ATP) competitive inhibitor of JNK, with a 300-fold selectivity of inhibition of JNK as compared with the extracellular signal-regulated kinases (ERKs) and p38 mitogen-activated protein kinases (MAPKs).<sup>52,53</sup> Spinal cord was isolated at 4h after injury,

and cytoplasmic fractioned spinal samples (S-100) were prepared. Western blot and quantitative analyses showed that SP600125 treatment significantly decreased the level of cytochrome c and caspase-9 when compared with vehicle control ( $n=3$ , Figs. 6A and B; vehicle,  $4.3 \pm 0.34$  vs. SP600125,  $2.9 \pm 0.25$  for cytochrome c; vehicle,  $4.7 \pm 0.45$  vs. SP600125,  $2.1 \pm 0.33$  for caspase-9,  $p < 0.05$ ). Several reports also show that JNK activation mediates cytochrome c release by inducing and promoting phosphorylation of Bim and Mcl-1.<sup>54-56</sup> Therefore, to examine the change of Mcl-1 and Bim phosphorylation at indicated time points (sham, 2h, 4h, 1 day, and 3 days) and the effect of SP600125 on its level at 4h after injury, spinal samples were prepared and processed for Western blot. Data showed that the level of Mcl-1 was progressively decreased, and that Bim was not changed after SCI, whereas the level of phosphorylated Bim and Mcl-1 was increased and peaked at 4h after injury (Figs. 6C and D). Furthermore, SP600125 significantly attenuated phosphorylation of Bim and Mcl-1 at 4h after injury ( $n=3$ , Figs. 6E and F; vehicle,  $1.0 \pm 0.09$  vs. SP600125,  $0.42 \pm 0.07$  for p-Mcl-1; vehicle,  $1.0 \pm 0.06$  vs. SP600125,  $0.68 \pm 0.05$  for p-Bim,  $p < 0.05$ ). These results, therefore, suggest that JNK activation mediates Bim and Mcl-1 phosphorylation, thereby inhibiting cytochrome c release after SCI.

#### VPA inhibits ER stress-associated caspase-12 activation after SCI

It is well known that apoptotic cell death is mediated by mitochondria-dependent signaling, thereby activating caspase-3 under oxidative stress.<sup>7,57</sup> In addition, ER stress-induced apoptotic cell death has also been implicated in many diseases including SCI.<sup>19,58-60</sup> Therefore, we next examined whether caspase-12, which is associated with ER stress-induced apoptotic cell death,<sup>21</sup> is activated after SCI, and whether VPA affects its activation. As shown in Figure 7A, the level of cleaved caspase-12 (26 kDa, active form) was markedly increased, and peaked 4h after injury as compared with sham control, and then decreased. Double immunofluorescence staining also showed that neurons, especially VMNs in the ventral horn, were positive for caspase-12 (Fig. 2B), whereas astrocytes and microglia were negative for caspase-12 (data not shown). Next, we examined whether VPA would affect caspase-12 activation after injury. Rats were given VPA (300 mg/kg) immediately after SCI, and spinal extracts were then prepared at 4h after injury. Western blot and quantitative analysis revealed that SCI-induced caspase-12 activation was significantly inhibited by VPA when compared with vehicle control ( $n=3$ , Fig. 7C; vehicle,  $12.4 \pm 0.55$  vs. VPA,  $6.3 \pm 0.43$  at 4h,  $p < 0.05$ ). By contrast, VPA treatment did not affect the level of active form of caspase-12 in uninjured spinal cord (data not shown). These results indicate that VPA inhibits ER stress-associated caspase-12 activation in the VMN after SCI.

#### VPA increases Bcl-2/Bax ratio by inhibiting CHOP expression after SCI

As cytochrome c release is known to be linked to Bcl-2 and/or Bax under ER stress,<sup>60-62</sup> we next examined the effect of VPA on Bcl-2 and Bax expression after SCI. Western blots showed that Bcl-2 expression was increased, whereas Bax expression was progressively decreased after injury as compared with sham controls (Fig. 8A). Furthermore, Bcl-2 expression was further increased by VPA, whereas Bax expression was not affected, which resulted in an increase in the Bcl-2/Bax ratio known as a rheostat, to determine cell susceptibility to apoptosis in many systems.<sup>63,64</sup>

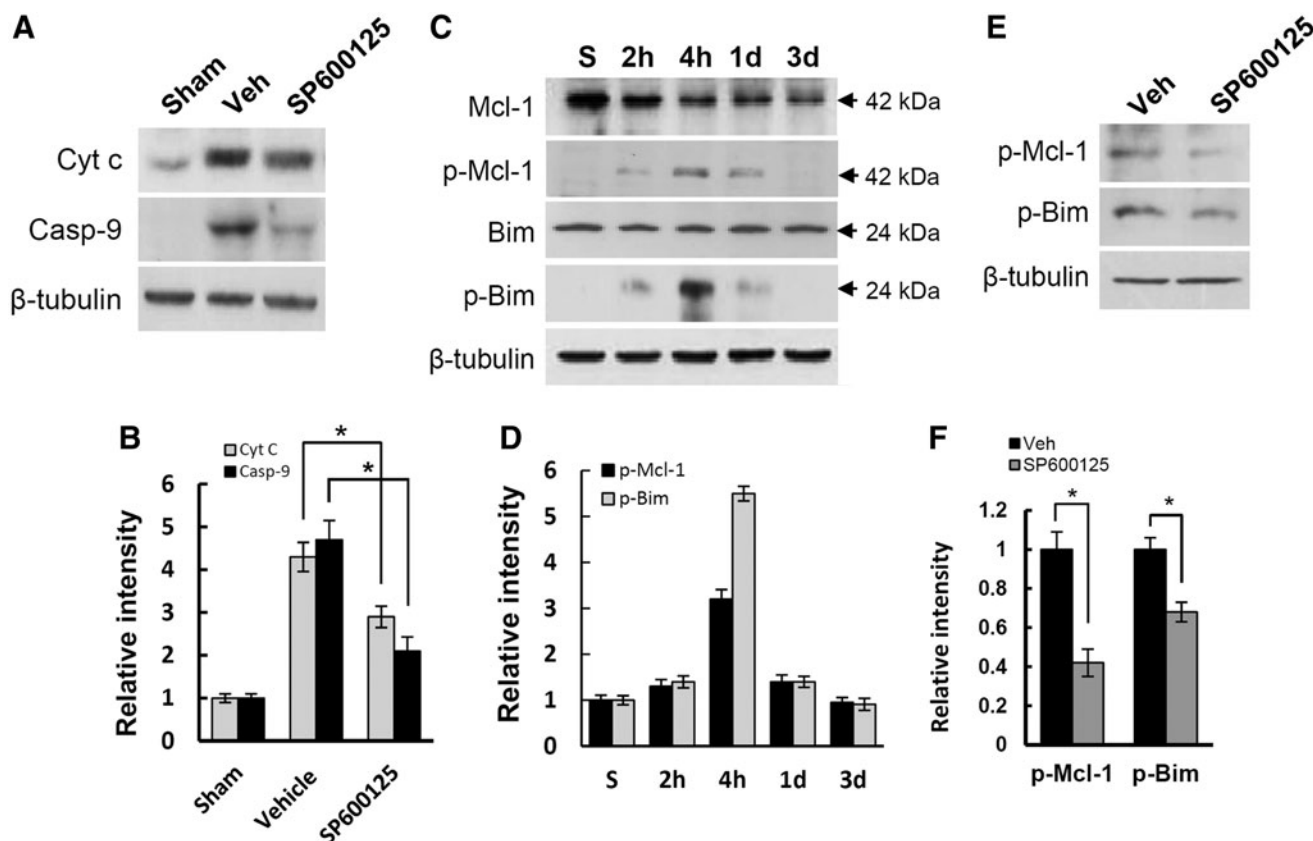


**FIG. 6.** c-Jun N-terminal kinase (JNK) activation induced cytochrome c release by Mcl-1 and Bim phosphorylation after spinal cord injury (SCI). S-100 and total proteins were prepared from spinal tissues treated with and not treated with valproic acid (VPA) and SP600125, a specific JNK inhibitor, at indicated time points after SCI, and Western blots of cytochrome c, Mcl-1, p-Mcl-1, Bim, and p-Bim were performed ( $n = 3/\text{group}$ ). Western blot (A) and quantification analysis (B) of cytochrome c and caspase-9 with S-100 (30  $\mu\text{g}$ ) at 4 h after injury ( $n = 3/\text{group}$ ). Note that cytochrome c release and caspase-9 activation were significantly inhibited by SP600125. Western blots (C) and quantification analysis (D) of Mcl-1, p-Mcl-1, Bim, and p-Bim with total protein (50  $\mu\text{g}$ ) prepared at 2 h, 4 h, 1 day, and 3 days after injury. Western blot (E) and quantification analysis (F) of p-Mcl-1 and p-Bim with total protein treated with and not treated with SP600125 at 4 h after injury. Note that SCI-induced increase of p-Mcl-1 and p-Bim level was significantly inhibited by SP600125. Data are presented as means  $\pm$  SD. \* $p < 0.05$ .

( $n = 3$ , Fig. 8B; vehicle,  $0.97 \pm 0.12$  vs. VPA,  $1.8 \pm 0.31$  at 4 h,  $p < 0.05$ ). As Bcl-2 expression is inhibited by CHOP expression under ER stress,<sup>65</sup> we also examined the effect of VPA on CHOP expression after injury. RT-PCR and Western blot analysis showed that the increase of SCI-induced CHOP expression at 4 h after injury was significantly alleviated by VPA ( $n = 3$ , Fig. 8C and D; vehicle,  $1.0 \pm 0.03$  vs. VPA,  $0.58 \pm 0.04$  for mRNA,  $p < 0.05$ ; vehicle,  $0.98 \pm 0.06$  vs. VPA,  $0.39 \pm 0.04$  for mRNA,  $p < 0.01$ ). These data suggest that VPA also inhibits cytochrome c release by increasing Bcl-2/Bax ratio through downregulation of CHOP expression after SCI. Finally, we examined the effect of VPA on caspase-3 activation at 4 h after SCI. Western blot and quantitative analysis showed that VPA treatment significantly decreased the level of activated caspase-3, as compared with vehicle control ( $n = 3$ , Fig. 8E and F; vehicle,  $3.9 \pm 0.2$  vs. VPA,  $1.9 \pm 0.2$ ,  $p < 0.01$ ).

## Discussion

Our recent study shows that VPA inhibits neuronal cell death after SCI by inhibiting BSCB disruption via inhibition of matrix metalloproteinase 9 (MMP-9) activity.<sup>30</sup> The present study demonstrated an additional mechanism of the neuroprotective effect of

VPA after SCI with an emphasis on oxidative stress and ER stress-mediated apoptotic cell death pathway. Our results showed that VPA treatment inhibited the activation of JNK pathway via inhibiting ROS production after SCI. In addition, we demonstrated that JNK activation in VMN after SCI contributed to cytochrome c release from mitochondria by increasing the phosphorylation of Mcl-1 and Bim. Furthermore, we showed that VPA also inhibited ER stress-associated caspase-12 activation in VMN, and that VPA increased Bcl-2/Bax ratio, which is known to be linked to cytochrome c release under ER stress, through downregulation of CHOP expression after SCI. Taken together, our data suggest that the neuroprotection by VPA is also in part mediated by inhibiting cytochrome c release under oxidative stress and ER stress after SCI (Fig. 9).

Oxidative stress has been implicated in the pathogenesis of selective VMN death in animal models of SCI and familial ALS.<sup>11,12,15</sup> In addition, the report by Guegan et al.<sup>12</sup> showed that VMN death is followed by mitochondrial cytochrome c release into the cytosol and concomitant with caspase-9 activation. In this study, the production of  $\text{O}_2^-$  was increased after SCI as in previous reports,<sup>7-10</sup> and VPA reduced  $\text{O}_2^-$  production (see Figs. 2A and B). In addition, VPA inhibited iNOS expression, which is known to

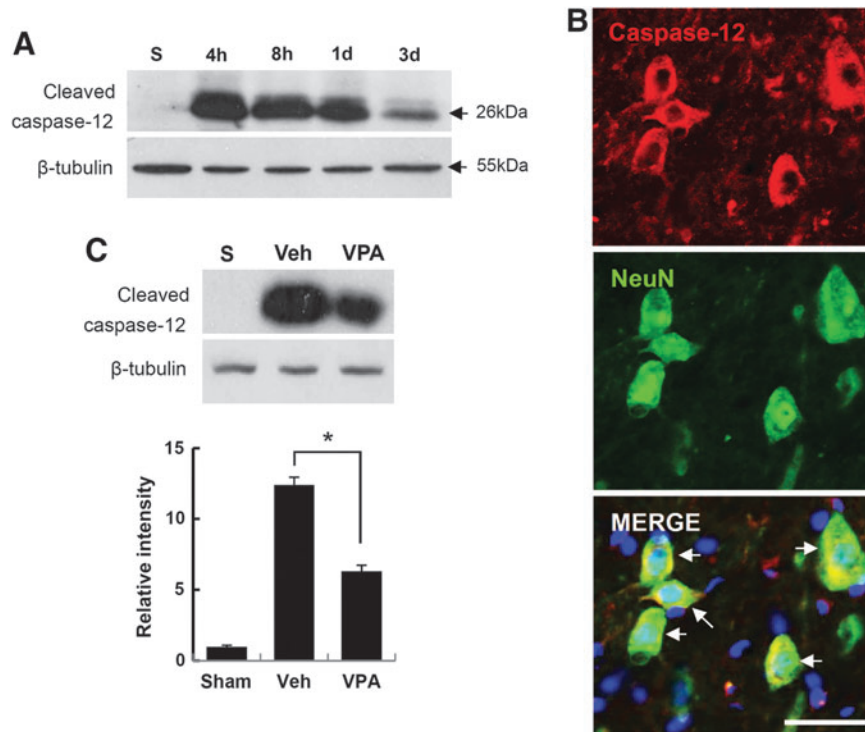


**FIG. 7.** Valproic acid (VPA) inhibits endoplasmic reticulum (ER) stress-associated caspase-12 activation after spinal cord injury. Spinal tissues and protein extracts given with and without VPA were prepared at the indicated time points (4h, 8h, 1 day, and 3 days after injury) as described in the Methods section ( $n=3/\text{group}$ ). Total protein ( $50\ \mu\text{g}$ ) was analyzed by sodium dodecyl sulfate (SDS)-polyacrylamide gel electrophoresis (PAGE) and subjected to Western blot with anti-cleaved caspase-12 antibody (A). Spinal tissues 1 mm rostral from lesion site prepared at 4h after injury were processed for double immunofluorescence staining with anti-caspase-12 and anti-NeuN antibodies (B). Note that cleaved caspase-12 was co-localized with neurons, especially ventral motor neurons (VMN) after SCI. Scale bar,  $30\ \mu\text{m}$ . (C) Western blot (upper) and quantitative analysis (bottom) of cleaved caspase-12 with total protein prepared at 4h after injury. Note that VPA significantly inhibited the level of cleaved caspase-12 as compared with vehicle control. Data are presented as means  $\pm$  SD.  $*p < 0.05$ . Color image is available online at [www.liebertpub.com/neu](http://www.liebertpub.com/neu)

induce and produce NO after SCI (see Figs. 2C and D). It is known that NO reacts with  $\text{O}_2^-$ , producing peroxynitrite, which results in lipid peroxidation and protein carbonylation and nitration.<sup>8,66</sup> In our study, VPA significantly inhibited both lipid peroxidation and protein nitration, which are increased after SCI (see Fig. 2E–I). In parallel, VPA significantly reduced VMN cell loss and cell death after SCI (see Fig. 1). Therefore, our results suggest that VPA exerts, in part, its neuroprotective effect via inhibition of ROS production, thereby reducing oxidative stress after SCI. However, the question for how VPA prevents ROS production after SCI remains, and should be investigated in future.

It is well known that JNK is activated under oxidative stress. Our data show that the level of p-JNK was increased in the VMN after SCI, and that MnTBAP treatment significantly decreased the levels of p-JNK and p-c-Jun, suggesting that ROS probably contribute to JNK activation after SCI (see Fig. 3). In addition, VPA inhibited JNK activation after SCI (see Fig. 4A). Therefore, these data suggest that VPA inhibited JNK activation in the VMN by reducing ROS production after SCI. Our data also show that the activated JNK mediated the phosphorylation of Bim, one of the pro-apoptotic Bcl-2 family proteins, and Mcl-1, one of the anti-apoptotic Bcl-2 family proteins. Furthermore, SP600125, a specific JNK inhibitor, inhibited phosphorylation of Bim and Mcl-1 (see Fig. 6E and F) and, therefore, our results are in agreement with other reports showing that JNK activation mediates cytochrome c release by inducing and promoting phosphorylation of Bim and Mcl-1.<sup>54–56</sup> It was also known that

JNK3 activated after SCI induces cytochrome c release by facilitating phosphorylation of Mcl-1,<sup>67</sup> which leads to degradation of Mcl-1 protein by proteasomal degradation.<sup>68</sup> Our data also showed that the level of Mcl-1 was decreased after SCI (Fig. 6C). Therefore, our data suggest that the attenuation of cytochrome c release by VPA may be mediated in part by the inhibition of the phosphorylation following degradation of Mcl-1, as well as Bim phosphorylation by JNK after SCI. Although it was known that glycogen synthase kinase 3 (GSK3) signaling mediates Mcl-1 phosphorylation following degradation through the ubiquitin-proteasome pathway, the involvement of GSK3 in Mcl-1 phosphorylation after SCI was not examined in this study, and will be investigated as a future study.

In addition to the mitochondria-dependent pathway, ER stress has received attention as an apoptotic regulatory pathway. Furthermore, mitochondrial dysfunction is closely linked to ER under ER stress.<sup>17,69</sup> It has been reported that UPR-related molecules such as Grp78 and CHOP were upregulated at an early stage after SCI.<sup>32</sup> In addition, the UPR ultimately triggered the apoptotic pathway under severe ER stress, and one of the important molecules relevant to cell death was caspase-12, which is regarded as a representative cell death signal.<sup>70,71</sup> Our data also showed that caspase-12 activation was markedly increased in neurons, especially in motor neurons in the ventral horn after SCI, which was significantly inhibited by VPA (see Fig. 7). It has been known that ER stress is linked to cytochrome c release from mitochondria

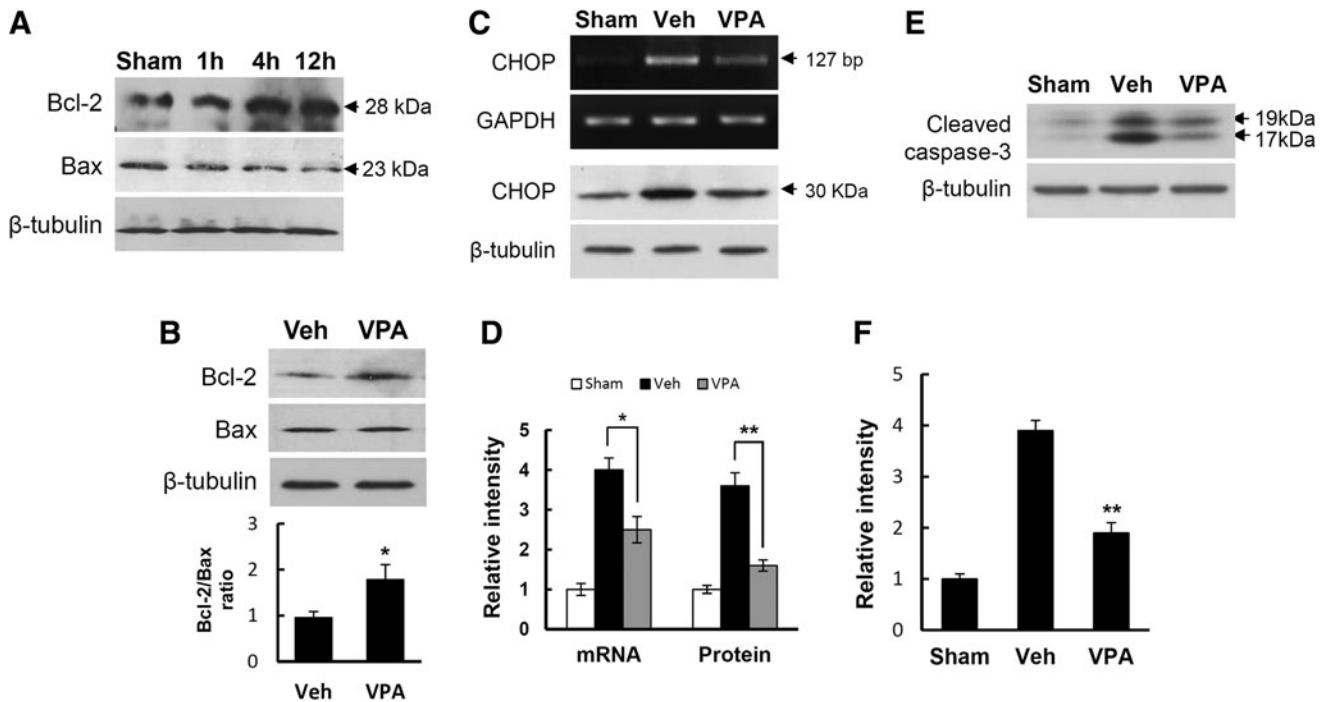


**FIG. 8.** Valproic acid (VPA) inhibits CHOP expression and increases Bcl-2/Bax ratio after spinal cord injury (SCI). Spinal samples prepared at indicated time points and from injured spinal cord treated with and not treated with VPA at 4 h after SCI were processed for reverse transcription polymerase chain reaction (RT-PCR) of CHOP and Western blot of Bcl-2, Bax, and caspase-3 with total protein (50  $\mu$ g) ( $n=3$ /group). (A,B) Western blots of Bcl-2 and Bax. Note that Bcl-2 was increased after SCI (A) and that Bcl-2/Bax ratio was significantly increased by VPA (B). (C,D) RT-PCR (C, upper), Western blot (C, lower), and quantification analysis (D) of CHOP expression. Note that VPA significantly inhibited CHOP expression after SCI. Western blot (E) and quantification analysis (F) of caspase-3. Note that caspase-3 activation after SCI was significantly inhibited by VPA. Values are mean  $\pm$  SD. \* $p < 0.05$ . \*\* $p < 0.01$ .

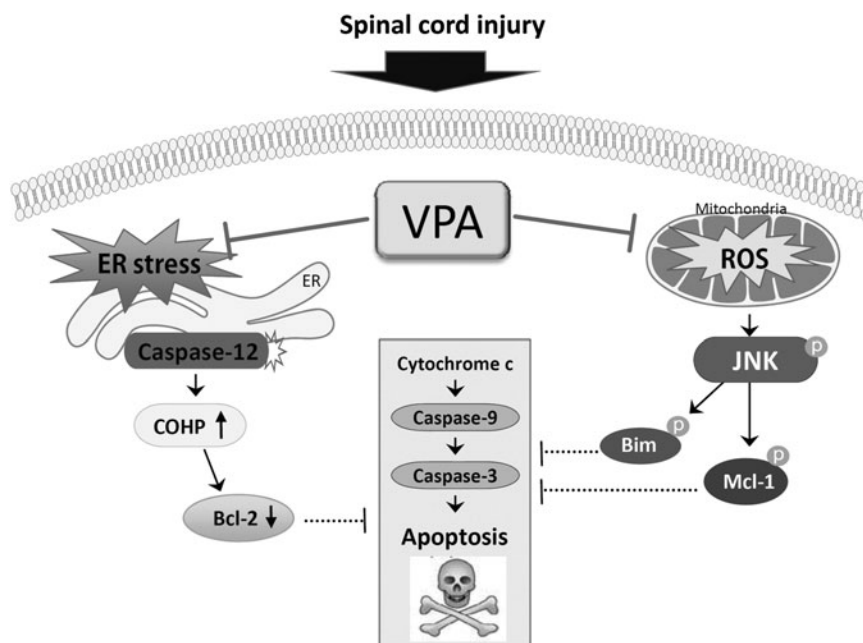


**FIG. 9.** Schematic diagram showing the neuroprotective effect of valproic acid (VPA) after SCI. Both endoplasmic reticulum (ER) stress-induced caspase-12 activation and reactive oxygen species (ROS)-mediated c-Jun N-terminal kinase (JNK) activation contributed to ventral motor neuron death after SCI, which was inhibited by VPA.

through the crosstalk between the Bcl-2 family proteins and the UPR,<sup>72</sup> and that activated caspase-12 interacts with caspase-9, which mediates the intrinsic apoptotic pathway, leading to caspase-3 activation.<sup>73</sup> Especially under ER stress, Bcl-2 expression was inhibited by CHOP expression, which leads to cytochrome c release.<sup>65</sup> In our data, VPA significantly increased Bcl-2/Bax ratio and inhibited CHOP expression (see Fig. 8A-D). In addition, caspase-3 activation was inhibited by VPA. Therefore, our data suggest that the attenuation of cytochrome c release by VPA was mediated by inhibition of CHOP expression, thereby increasing the Bcl-2/Bax ratio. Taken together, our results suggest that the neuroprotective effect of VPA after SCI may be mediated in part by inhibiting the ER stress-induced apoptotic pathway.

VPA is well known to inhibit histone deacetylase (HDAC) at therapeutic levels (with a half maximal inhibitory concentration [IC<sub>50</sub>]=0.4 mM), causing histone hyperacetylation.<sup>74,75</sup> HDAC is also implicated in the modulation of gene expression as well as in the life span in a variety of organisms such as yeast, *Caenorhabditis elegans* and *Drosophila*.<sup>76</sup> Therefore, we cannot rule out the possibility that the effect of VPA might be processed under epigenetic control, and that further experiments to uncover epigenetic control mechanisms by VPA are necessary.

## Conclusion

In summary, our results indicate that in addition to the inhibition of BSCB disruption by VPA after SCI,<sup>30</sup> the inhibition of mitochondrial cytochrome c release following apoptotic signaling pathways by VPA under both oxidative stress and ER stress after injury may account, in part, for its neuroprotective effect. Taken together, our findings thus demonstrate that the cellular and molecular mechanisms underlying neuroprotection by VPA after SCI appear to be multifaceted. Our study suggests the possibility that VPA is a potential therapeutic agent after SCI, as the drug is already in clinical use.

## Acknowledgments

This research was supported by National Research Foundation of Korea funded by the Ministry of Science, Information and Communications Technology & Future Planning (No. 2010-0019349 [Pioneer Research Center Program], No. 2008-0061888 [Science Research Center]) and a grant from the Korea Health Technology R&D Project, Ministry of Health & Welfare, Republic of Korea (A101198).

## Author Disclosure Statement

No competing financial interests exist.

## References

- Liu, X.Z., Xu, X. M., Hu, R., Du, C., Zhang, S.X., McDonald, J.W., Dong, H.X., Wu, Y.J., Fan, G.S., Jacquin, M.F., Hsu, C.Y., and Choi, D.W. (1997). Neuronal and glial apoptosis after traumatic spinal cord injury. *J. Neurosci.* 17, 5395–5406.
- Tator, C.H., and Fehlings, M.G. (1991). Review of the secondary injury theory of acute spinal cord trauma with emphasis on vascular mechanisms. *J. Neurosurg.* 75, 15–26.
- Emery, E., Aldana, P., Bunge, M.B., Puckett, W., Srinivasan, A., Keane, R.W., Bethea, J., and Levi, A.D. (1998). Apoptosis after traumatic human spinal cord injury. *J. Neurosurg.* 89, 911–920.
- Grossman, S.D., Rosenberg, L.J., and Wrathall, J.R. (2001). Temporal-spatial pattern of acute neuronal and glial loss after spinal cord contusion. *Exp. Neurol.* 168, 273–282.
- Tomiya, M., Kimura, T., Maeda, T., Tanaka, H., Furusawa, K., Kurahashi, K., and Matsunaga, M. (2001). Expression of metabotropic

- glutamate receptor mRNAs in the human spinal cord: implications for selective vulnerability of spinal motor neurons in amyotrophic lateral sclerosis. *J. Neurol. Sci.* 189, 65–69.
- Wengenack, T.M., Holasek, S.S., Montano, C.M., Gregor, D., Curran, G.L., and Poduslo, J.F. (2004). Activation of programmed cell death markers in ventral horn motor neurons during early presymptomatic stages of amyotrophic lateral sclerosis in a transgenic mouse model. *Brain Res.* 1027, 73–86.
- Xu, W., Chi, L., Xu, R., Ke, Y., Luo, C., Cai, J., Qiu, M., Gozal, D., and Liu, R. (2005). Increased production of reactive oxygen species contributes to motor neuron death in a compression mouse model of spinal cord injury. *Spinal Cord.* 43, 204–213.
- Yune, T.Y., Chang, M.J., Kim, S.J., Lee, Y.B., Shin, S.W., Rhim, H., Kim, Y.C., Shin, M.L., Oh, Y.J., Han, C.T., Markelonis, G.J., and Oh, T.H. (2003). Increased production of tumor necrosis factor- $\alpha$  induces apoptosis after traumatic spinal cord injury in rats. *J. Neurotrauma* 20, 207–219.
- Mu, X., Azbill, R.D., and Springer, J.E. (2002). NBQX treatment improves mitochondrial function and reduces oxidative events after spinal cord injury. *J. Neurotrauma* 19, 917–927.
- Conti, A., Miscusi, M., Cardali, S., Germano, A., Suzuki, H., Cuzocrea, S., and Tomasello, F. (2007). Nitric oxide in the injured spinal cord: synthases cross-talk, oxidative stress and inflammation. *Brain Res. Rev.* 54, 205–218.
- Liu, D., Sybert, T.E., Qian, H., and Liu, J. (1998). Superoxide production after spinal injury detected by microperfusion of cytochrome c. *Free Radic. Biol. Med.* 25, 298–304.
- Guegan, C., Vila, M., Rosoklija, G., Hays, A.P., and Przedborski, S. (2001). Recruitment of the mitochondrial-dependent apoptotic pathway in amyotrophic lateral sclerosis. *J. Neurosci.* 21, 6569–6576.
- Wang, G.H., Jiang, Z.L., Li, Y.C., Li, X., Shi, H., Gao, Y.Q., Vosler, P.S., and Chen, J. (2011). Free-radical scavenger edaravone treatment confers neuroprotection against traumatic brain injury in rats. *J. Neurotrauma* 28, 2123–2134.
- Raza, S.S., Khan, M.M., Ashafaq, M., Ahmad, A., Khuwaja, G., Khan, A., Siddiqui, M.S., Safhi, M.M., and Islam, F. (2011). Silymarin protects neurons from oxidative stress associated damages in focal cerebral ischemia: a behavioral, biochemical and immunohistological study in Wistar rats. *J. Neurol. Sci.* 309, 45–54.
- Yune, T.Y., Lee, J.Y., Jiang, M.H., Kim, D.W., Choi, S.Y., and Oh, T.H. (2008). Systemic administration of PEP-1-SOD1 fusion protein improves functional recovery by inhibition of neuronal cell death after spinal cord injury. *Free Radic. Biol. Med.* 45, 1190–1200.
- Sugawara, T., Lewen, A., Gasche, Y., Yu, F., and Chan, P.H. (2002). Overexpression of SOD1 protects vulnerable motor neurons after spinal cord injury by attenuating mitochondrial cytochrome c release. *FASEB J.* 16, 1997–1999.
- Rao, R.V., Hermel, E., Castro-Oregon, S., del, R.G., Ellerby, L. M., Ellerby, H.M., and Bredesen, D.E. (2001). Coupling endoplasmic reticulum stress to the cell death program. Mechanism of caspase activation. *J. Biol. Chem.* 276, 33,869–33,874.
- Oyadomari, S. and Mori, M. (2004). Roles of CHOP/GADD153 in endoplasmic reticulum stress. *Cell Death Differ.* 11, 381–389.
- Penas, C., Guzman, M. S., Verdu, E., Fores, J., Navarro, X., and Casas, C. (2007). Spinal cord injury induces endoplasmic reticulum stress with different cell-type dependent response. *J. Neurochem.* 102, 1242–1255.
- Yamauchi, T., Sakurai, M., Abe, K., Matsumiya, G., and Sawa, Y. (2007). Impact of the endoplasmic reticulum stress response in spinal cord after transient ischemia. *Brain Res.* 1169, 24–33.
- Sakurai, M., Takahashi, G., Abe, K., Horinouchi, T., Itoyama, Y., and Tabayashi, K. (2005). Endoplasmic reticulum stress induced in motor neurons by transient spinal cord ischemia in rabbits. *J. Thorac. Cardiovasc. Surg.* 130, 640–645.
- Bravo, R., Gutierrez, T., Paredes, F., Gatica, D., Rodriguez, A.E., Pedrozo, Z., Chiong, M., Parra, V., Quest, A.F., Rothermel, B.A., and Lavandero, S. (2012). Endoplasmic reticulum: ER stress regulates mitochondrial bioenergetics. *Int. J. Biochem. Cell Biol.* 44, 16–20.
- Verfaillie, T., Rubio, N., Garg, A.D., Bultynck, G., Rizzuto, R., Decuyper, J.P., Piette, J., Linehan, C., Gupta, S., Samali, A., and Agostinis, P. (2012). PERK is required at the ER-mitochondrial contact sites to convey apoptosis after ROS-based ER stress. *Cell Death Differ.* 19, 1880–1891.
- Johannessen, C.U. (2000). Mechanisms of action of valproate: a commentary. *Neurochem. Int.* 37, 103–110.

25. Tunnicliff, G. (1999). Actions of sodium valproate on the central nervous system. *J. Physiol. Pharmacol.* 50, 347–365.
26. Qian, Y.R., Lee, M.J., Hwang, S., Kook, J.H., Kim, J.K., and Bae, C.S. (2010). Neuroprotection by valproic acid in mouse models of permanent and transient focal cerebral ischemia. *Korean J. Physiol. Pharmacol.* 14, 435–440.
27. Kim, H.J., Rowe, M., Ren, M., Hong, J.S., Chen, P.S., and Chuang, D.M. (2007). Histone deacetylase inhibitors exhibit anti-inflammatory and neuroprotective effects in a rat permanent ischemic model of stroke: multiple mechanisms of action. *J. Pharmacol. Exp. Ther.* 321, 892–901.
28. Tsai, L.K., Tsai, M.S., Ting, C.H., and Li, H. (2008). Multiple therapeutic effects of valproic acid in spinal muscular atrophy model mice. *J. Mol. Med. (Berl)* 86, 1243–1254.
29. Feng, L., Tang, W.W., Loskutoff, D.J., and Wilson, C.B. (1993). Dysfunction of glomerular fibrinolysis in experimental antiglomerular basement membrane antibody glomerulonephritis. *J. Am. Soc. Nephrol.* 3, 1753–1764.
30. Lee, J.Y., Kim, H.S., Choi, H.Y., Oh, T.H., Ju, B.G., and Yune, T.Y. (2012). Valproic acid attenuates blood–spinal cord barrier disruption by inhibiting matrix metalloproteinase-9 activity and improves functional recovery after spinal cord injury. *J. Neurochem.* 121, 818–829.
31. Lv, L., Sun, Y., Han, X., Xu, C.C., Tang, Y.P., and Dong, Q. (2011). Valproic acid improves outcome after rodent spinal cord injury: Potential roles of histone deacetylase inhibition. *Brain Res.* 1396, 60–68.
32. Penas, C., Verdu, E., Sensio-Pinilla, E., Guzman-Lenis, M.S., Herando-Grabulosa, M., Navarro, X., and Casas, C. (2011). Valproate reduces CHOP levels and preserves oligodendrocytes and axons after spinal cord injury. *Neuroscience* 178, 33–44.
33. Lee, J.Y., Chung, H., Yoo, Y.S., Oh, Y.J., Oh, T.H., Park, S., and Yune, T.Y. (2010). Inhibition of apoptotic cell death by ghrelin improves functional recovery after spinal cord injury. *Endocrinology* 151, 3815–3826.
34. Wang, X.W., Hu, S., Mao-Ying, Q.L., Li, Q., Yang, C.J., Zhang, H., Mi, W.L., Wu, G.C., and Wang, Y.Q. (2012). Activation of c-jun N-terminal kinase in spinal cord contributes to breast cancer induced bone pain in rats. *Mol. Brain* 5, 21.
35. Choi, D.C., Lee, J.Y., Lim, E.J., Baik, H.H., Oh, T.H., and Yune, T.Y. (2012). Inhibition of ROS-induced p38MAPK and ERK activation in microglia by acupuncture relieves neuropathic pain after spinal cord injury in rats. *Exp. Neurol.* 236, 268–282.
36. Yune, T.Y., Park, H.G., Lee, J.Y., and Oh, T.H. (2008). Estrogen-Induced Bcl-2 Expression after Spinal Cord Injury Is Mediated through Phosphoinositide-3-Kinase/Akt-Dependent CREB Activation. *J. Neurotrauma* 25, 1121–1131.
37. Noble, L.J. and Wrathall, J.R. (1985). Spinal cord contusion in the rat: morphometric analyses of alterations in the spinal cord. *Exp. Neurol.* 88, 135–149.
38. Bindokas, V.P., Jordan, J., Lee, C.C., and Miller, R.J. (1996). Superoxide production in rat hippocampal neurons: selective imaging with hydroethidine. *J. Neurosci.* 16, 1324–1336.
39. Yune, T.Y., Lee, J.Y., Jung, G.Y., Kim, S.J., Jiang, M.H., Kim, Y.C., Oh, Y.J., Markelonis, G.J., and Oh, T.H. (2007). Minocycline alleviates death of oligodendrocytes by inhibiting pro-nerve growth factor production in microglia after spinal cord injury. *J. Neurosci.* 27, 7751–7761.
40. Yune, T.Y., Lee, S.M., Kim, S.J., Park, H.K., Oh, Y.J., Kim, Y.C., Markelonis, G.J., and Oh, T.H. (2004). Manganese superoxide dismutase induced by TNF-beta is regulated transcriptionally by NF-kappaB after spinal cord injury in rats. *J. Neurotrauma* 21, 1778–1794.
41. Wang, J.F., Azzam, J.E., and Young, L.T. (2003). Valproate inhibits oxidative damage to lipid and protein in primary cultured rat cerebrocortical cells. *Neuroscience* 116, 485–489.
42. Moon, Y.J., Lee, J.Y., Oh, M.S., Pak, Y.K., Park, K.S., Oh, T.H., and Yune, T.Y. (2012). Inhibition of inflammation and oxidative stress by *Angelica dahuricae* radix extract decreases apoptotic cell death and improves functional recovery after spinal cord injury. *J. Neurosci. Res.* 90, 243–256.
43. Valko, M., Leibfritz, D., Moncol, J., Cronin, M.T., Mazur, M., and Telsler, J. (2007). Free radicals and antioxidants in normal physiological functions and human disease. *Int. J. Biochem. Cell Biol.* 39, 44–84.
44. Zhu, X., Raina, A.K., Lee, H.G., Chao, M., Nunomura, A., Tabaton, M., Petersen, R.B., Perry, G., and Smith, M.A. (2003). Oxidative stress and neuronal adaptation in Alzheimer disease: the role of SAPK pathways. *Antioxid. Redox. Signal.* 5, 571–576.
45. Fiorillo, C., Becatti, M., Pensalfini, A., Cecchi, C., Lanzilao, L., Donzelli, G., Nassi, N., Giannini, L., Borchi, E., and Nassi, P. (2008). Curcumin protects cardiac cells against ischemia-reperfusion injury: effects on oxidative stress, NF-kappaB, and JNK pathways. *Free Radic. Biol. Med.* 45, 839–846.
46. Nakahara, S., Yone, K., Sakou, T., Wada, S., Nagamine, T., Niyama, T., and Ichijo, H. (1999). Induction of apoptosis signal regulating kinase 1 (ASK1) after spinal cord injury in rats: possible involvement of ASK1-JNK and -p38 pathways in neuronal apoptosis. *J. Neuro-pathol. Exp. Neurol.* 58, 442–450.
47. Yin, K.J., Kim, G.M., Lee, J.M., He, Y.Y., Xu, J., and Hsu, C.Y. (2005). JNK activation contributes to DP5 induction and apoptosis following traumatic spinal cord injury. *Neurobiol. Dis.* 20, 881–889.
48. Citron, B.A., Arnold, P.M., Sebastian, C., Qin, F., Malladi, S., Ameenuddin, S., Landis, M.E., and Festoff, B.W. (2000). Rapid up-regulation of caspase-3 in rat spinal cord after injury: mRNA, protein, and cellular localization correlates with apoptotic cell death. *Exp. Neurol.* 166, 213–226.
49. Springer, J.E., Azbill, R.D. and Knapp, P.E. (1999). Activation of the caspase-3 apoptotic cascade in traumatic spinal cord injury. *Nat. Med.* 5, 943–946.
50. Gao, Y., Signore, A.P., Yin, W., Cao, G., Yin, X.M., Sun, F., Luo, Y., Graham, S.H., and Chen, J. (2005). Neuroprotection against focal ischemic brain injury by inhibition of c-Jun N-terminal kinase and attenuation of the mitochondrial apoptosis-signaling pathway. *J. Cereb. Blood Flow Metab.* 25, 694–712.
51. Guan, Q.H., Pei, D.S., Liu, X.M., Wang, X.T., Xu, T.L., and Zhang, G.Y. (2006). Neuroprotection against ischemic brain injury by SP600125 via suppressing the extrinsic and intrinsic pathways of apoptosis. *Brain Res.* 1092, 36–46.
52. Wang, Y., Ji, H.X., Xing, S.H., Pei, D.S., and Guan, Q.H. (2007). SP600125, a selective JNK inhibitor, protects ischemic renal injury via suppressing the extrinsic pathways of apoptosis. *Life Sci.* 80, 2067–2075.
53. Bennett, B.L., Sasaki, D.T., Murray, B.W., O’Leary, E.C., Sakata, S.T., Xu, W., Leisten, J.C., Motiwala, A., Pierce, S., Satoh, Y., Bhagwat, S.S., Manning, A.M., and Anderson, D.W. (2001). SP600125, an anthrapyrazolone inhibitor of Jun N-terminal kinase. *Proc. Natl. Acad. Sci. U. S. A.* 98, 13,681–13,686.
54. Inoshita, S., Takeda, K., Hatai, T., Terada, Y., Sano, M., Hata, J., Umezawa, A., and Ichijo, H. (2002). Phosphorylation and inactivation of myeloid cell leukemia 1 by JNK in response to oxidative stress. *J. Biol. Chem.* 277, 43,730–43,734.
55. Lei, K., and Davis, R.J. (2003). JNK phosphorylation of Bim-related members of the Bcl2 family induces Bax-dependent apoptosis. *Proc. Natl. Acad. Sci. U. S. A.* 100, 2432–2437.
56. Putcha, G.V., Le, S., Frank, S., Besirli, C.G., Clark, K., Chu, B., Alix, S., Youle, R.J., LaMarche, A., Maroney, A.C., and Johnson, Jr, E.M. (2003). JNK-mediated BIM phosphorylation potentiates BAX-dependent apoptosis. *Neuron* 38, 899–914.
57. Niizuma, K., Endo, H., and Chan, P.H. (2009). Oxidative stress and mitochondrial dysfunction as determinants of ischemic neuronal death and survival. *J. Neurochem.* 109, Suppl. 1, 133–138.
58. Boyce, M., and Yuan, J. (2006). Cellular response to endoplasmic reticulum stress: a matter of life or death. *Cell Death Differ.* 13, 363–373.
59. Lindholm, D., Wootz, H., and Korhonen, L. (2006). ER stress and neurodegenerative diseases. *Cell Death Differ.* 13, 385–392.
60. Arduino, D.M., Esteves, A.R., Domingues, A.F., Pereira, C.M., Cardoso, S.M., and Oliveira, C.R. (2009). ER-mediated stress induces mitochondrial-dependent caspases activation in NT2 neuron-like cells. *BMB Rep.* 42, 719–724.
61. Hacki, J., Egger, L., Monney, L., Conus, S., Rosse, T., Fellay, I., and Borner, C. (2000). Apoptotic crosstalk between the endoplasmic reticulum and mitochondria controlled by Bcl-2. *Oncogene* 19, 2286–2295.
62. Zhang, D., and Armstrong, J.S. (2007). Bax and the mitochondrial permeability transition cooperate in the release of cytochrome c during endoplasmic reticulum-stress-induced apoptosis. *Cell Death Differ.* 14, 703–715.
63. Korsmeyer, S.J. (1999). BCL-2 gene family and the regulation of programmed cell death. *Cancer Res.* 59, 1693s–1700s.

64. Oltvai, Z.N., Millman, C.L., and Korsmeyer, S.J. (1993). Bcl-2 heterodimerizes in vivo with a conserved homolog, Bax, that accelerates programmed cell death. *Cell* 74, 609–619.
65. McCullough, K.D., Martindale, J.L., Klotz, L.O., Aw, T.Y., and Holbrook, N.J. (2001). Gadd153 sensitizes cells to endoplasmic reticulum stress by down-regulating Bcl2 and perturbing the cellular redox state. *Mol. Cell Biol.* 21, 1249–1259.
66. Bao, F., and Liu, D. (2002). Peroxynitrite generated in the rat spinal cord induces neuron death and neurological deficits. *Neuroscience* 115, 839–849.
67. Li, Q.M., Tep, C., Yune, T.Y., Zhou, X.Z., Uchida, T., Lu, K.P., and Yoon, S.O. (2007). Opposite regulation of oligodendrocyte apoptosis by JNK3 and Pin1 after spinal cord injury. *J. Neurosci.* 27, 8395–8404.
68. Morel, C., Carlson, S.M., White, F.M., and Davis, R.J. (2009). Mcl-1 integrates the opposing actions of signaling pathways that mediate survival and apoptosis. *Mol. Cell Biol.* 29, 3845–3852.
69. Orrenius, S., Zhivotovsky, B., and Nicotera, P. (2003). Regulation of cell death: the calcium-apoptosis link. *Nat. Rev. Mol. Cell Biol.* 4, 552–565.
70. Nakagawa, T., Zhu, H., Morishima, N., Li, E., Xu, J., Yankner, B. A., and Yuan, J. (2000). Caspase-12 mediates endoplasmic-reticulum-specific apoptosis and cytotoxicity by amyloid-beta. *Nature* 403, 98–103.
71. Oyadomari, S., Araki, E. and Mori, M. (2002). Endoplasmic reticulum stress-mediated apoptosis in pancreatic beta-cells. *Apoptosis* 7, 335–345.
72. Rodriguez, D., Rojas-Rivera, D., and Hetz, C. (2011). Integrating stress signals at the endoplasmic reticulum: The BCL-2 protein family rheostat. *Biochim. Biophys. Acta* 1813, 564–574.
73. Groenendyk, J., and Michalak, M. (2005). Endoplasmic reticulum quality control and apoptosis. *Acta Biochim. Pol.* 52, 381–395.
74. Phiel, C.J., Zhang, F., Huang, E.Y., Guenther, M.G., Lazar, M.A., and Klein, P.S. (2001). Histone deacetylase is a direct target of valproic acid, a potent anticonvulsant, mood stabilizer, and teratogen. *J Biol. Chem.* 276, 36,734–36,741.
75. Gottlicher, M., Minucci, S., Zhu, P., Kramer, O.H., Schimpf, A., Giavara, S., Sleeman, J.P., Lo, C.F., Nervi, C., Pelicci, P.G., and Heinzl, T. (2001). Valproic acid defines a novel class of HDAC inhibitors inducing differentiation of transformed cells. *EMBO J.* 20, 6969–6978.
76. Chang, K.T., and Min, K.T. (2002). Regulation of lifespan by histone deacetylase. *Ageing Res. Rev.* 1, 313–326.

Address correspondence to:

*Tae Y. Yune, PhD*

*Kyunghee University*

*Age-Related and Brain Diseases Research Center*

*Medical Building 10th Floor*

*Dongdaemun-gu, Hoegi-dong 1*

*Seoul 130-701*

*Republic of Korea*

*E-mail: tyune@khu.ac.kr*